

Time-dependent modelling and experimental validation of the metal/flux interface in a continuous casting mould

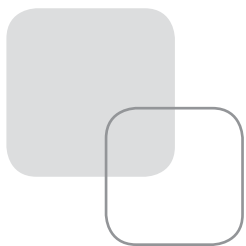
A complete fluid dynamics model of the continuous caster mould region, including the dynamic behaviour of the slag/steel interface, has been developed by solving the source-balance transport equations for conservation of mass, momentum and turbulence kinetic energy. The model is validated against a water/oil physical model equipped with LDA velocity measurements and video recordings of interface position.

■ ABSTRACT

This work concerns the development of a finite volume computer model of the continuous casting process for steel flat products. In this first stage, the model concentrates on the hydrodynamic aspects of the process and in particular the dynamic behaviour of the metal/slag interface. Instability and wave action observed at the interface has a bearing on the entrainment of inclusions into the melt and therefore it is important in the eventual quality of the product. This instability is due to the action of the submerged entry nozzle (SEN) jets, bringing the metal into the mould. Interface turbulence, wave behaviour and in fact the whole hydrodynamic picture in the mould region is also affected by the presence of argon bubbles which add buoyancy to the SEN jets. These are the features that need to be represented accurately in the model.

For any model to be successful it has to be representative of reality. As it is notoriously difficult to compare flow features against a real, operational caster, the model was validated against experimental measurements obtained in a water model apparatus at ArcelorMittal Research in Maizières. To represent the lighter layer, silicon oil was used and air was pumped through the SEN to represent the argon. LDA measurements were taken for different water flow rates and oil layer thicknesses and videos of the interface motion were made. FFT analysis of the experimental results identified distinct low frequency oscillations, thought to be associated with slow alternating oscillation of the two opposing SEN jets.

The CFD code PHYSICA was used to model the mould region. To retain the sharp interface between oil and water over a long simulation time, necessary to model low frequencies, a new implicit discontinuity tracking algorithm was developed, called the Counter Diffusion Method, or CDM. Turbulence was represented using a filtered version of the k- ϵ model, suitable for time-dependent simulations, with a density stratification term used to represent interface turbulence damping. Air bubbles were modelled using a Lagrangian tracking scheme, with two-way momentum feedback between the continuous and discrete phases effected through a mixture density modification. The simulations capture successfully the main characteristics of the flow, including its low frequency behaviour, and highlight flow modifications caused by the buoyancy effect of the bubbles.



■ INTRODUCTION

This work is part of a continuing PhD research programme and concerns the development of a complete model of the mould region of the continuous caster for steel plate products. The programme of research encompasses (a) fluid dynamics aspects and slag/interface motion, (b) heat transfer and solidification, (c) mass transfer and chemical reaction at the slag/metal interface. This contribution reports work on part (a) of the project, concentrating on fluid dynamics in the mould region.

The flow development that results from the action of the Submerged Entry Nozzle (SEN) that delivers the metal from the tundish to the mould is a subject of considerable interest in the research community (e.g. see Thomas (1)). The flow field is important as it determines the heat transfer in this region and the initial formation of the plate shell. The twin SEN jets, direct hot metal towards the long ends of the plate and once they reach the mould wall they are quenched first by contact with the water-cooled copper mould surface and further downstream by water cooling sprays. The Reynolds numbers involved are such that the flow in this top region is invariably turbulent which again has a considerable influence on how heat is distributed in the melt. As it is shown by water model experiments (2) and other numerical simulations (3, 4, 5), the jets are diverted at the wall to form two recirculation loops, a deep loop in the casting direction and a short upper loop which returns flow along the flux metal interface towards the SEN wall. Control of these loops is important in the continuous casting process as it determines the transport of inclusions (oxide impurities, gas bubbles, slag droplets) and into the solidifying skin leading to defects.

To prevent nozzle blocking, argon gas is injected into the SEN together with the liquid metal and the presence of these gas bubbles leads to additional effects: they add buoyancy to the jets altering the upper jet loop, they encourage mixing of the slag with the steel at the interface, and they act as carriers of inclusions. The flow computation needs to account for these bubbles, the result being a three-phase calculation (4).

The slag metal interface itself has a dynamic character since the 1:4 density ratio across it encourages the development of gravity waves. These waves are present even with a stationary mould and they appear to be excited by the SEN jets and also by the presence of gas bubbles (4). Water/oil experiments show (2) that the behaviour of the interface depends on

both gas and liquid flow rate, and suggest that large water flow rates may uncover part of the steel surface, close to the narrow ends of the mould. The experiments also suggest that SEN jet momentum is reduced as gas flow rate increases and mixing at the slag metal interface becomes more rigorous. In this paper an attempt is made to capture these complex effects in a simple multi-physics simulation. The water/oil LDA and video capture experiments at ArcelorMittal Research are used to validate the computer model.

■ EXPERIMENTAL SETUP

The water model

Data were obtained in an experimental water model rig (fig. 1). The experimental rig has an adaptable geometry which allows the testing of different dimensions of the mould and various SEN designs. Both mould and SEN are transparent and they are located in a robust support. Water circulation is provided by a pump that draws water from the collector at the bottom of the mould and pushes it into the tundish located

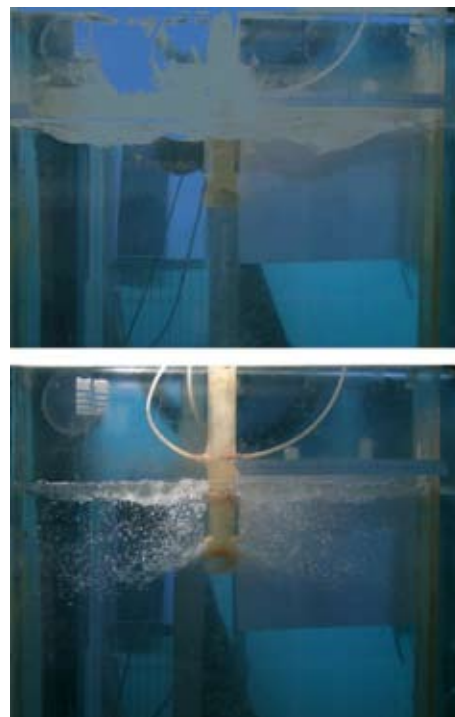


Fig. 1 - Video stills of the water-model experiment with and without gas (ArcelorMittal Research, 2005).

at the top of the mould. Different flow rates can easily be set. The system is also provided with electronic control for the immersion depth of the SEN. Measurements are taken using the LDA technique.

In the experiment silicon oil was used to mimic the slag layer and air was pumped through the SEN to mimic argon gas. Data were then collected for different water and gas flow rates and for different oil layer thickness. Horizontal velocity and its distribution in time were monitored in 15 experimental points along the middle plane of the mould.

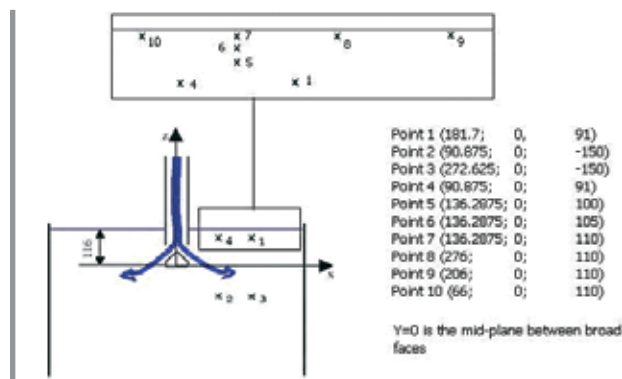


Fig. 2 - Experimental measurement arrangement.

Data Analysis

Using this setup, experimental data were collected at the specific points, shown in figure 2. Of the 10 points displayed, only numbers 1-5 were usable, as the others were too close to the moving interface.

In order to compare the experimental data against simulations a certain amount of manipulation was necessary:

- The data had to be filtered to remove high frequency spikes which are unlikely to have a hydrodynamic source;
- Averaged to determine the mean value of the signal and then;
- The average subtracted before a spectral analysis could be carried out.

Figure 3 shows the difference between the filtered and raw LDA signals. The raw signals exhibit peaks of 1m/s but with duration of 1ms or less, unlikely for a fluid with inertia, so these signals were excluded from subsequent frequency analysis by the filtering process. Various filter sizes were tested and the filtered signal with a base of 2 s is shown in the lower part of figure 3.

MATHEMATICAL MODEL

The simulation of the casting process models the continuum as a mixture of liquid/solid metal, molten flux and argon bubbles. In this three-phase simulation a Lagrangian particle-tracking algorithm is used to predict the motion of the argon

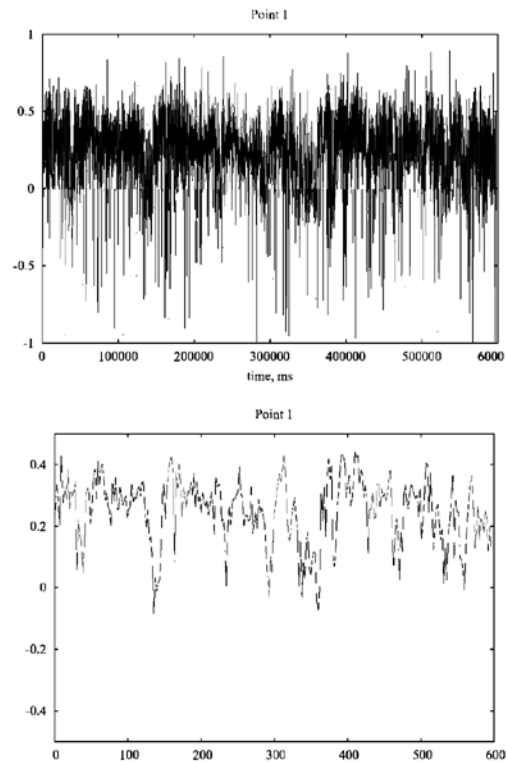


Fig. 3 - Comparison of raw and filtered signals from point 1 with a filter base of 2 s.

bubbles. Coupling between the mean flow and the bubbles is achieved through density variations in elements containing argon. Phase change within the metal is modelled through an enthalpy source-based method. The position of the interface between the metal and the molten flux is computed using an implicit VOF type method, optimized for speed using a counter-diffusion interface sharpening algorithm. The resulting flow field is turbulent with turbulence represented via an effective viscosity derived from a k-ε model formulation. The k-ε model is itself filtered to account for the time stepping nature of the calculation as explained below.

The finite volume method is used to discretise the governing equations in an unstructured centre-located scheme and the resulting linear system of equations is solved iteratively within the home-grown code PHYSICA (6). The equations used are described in the remainder of this section.

Momentum and Continuity

The conservation equations for momentum and mass for three dimensional fluid flow expressed in vector notation are:

$$\frac{\partial}{\partial t}(\rho \underline{u}) + \nabla \cdot (\rho \underline{u} \underline{u}) = \nabla \cdot (\mu \nabla \underline{u}) - \nabla p + \underline{S} \quad [1]$$

$$\frac{\partial \rho}{\partial t} + \nabla \cdot (\rho \underline{u}) = 0 \quad [2]$$

where \underline{u} is the velocity vector, p is the pressure, ρ is the mixture density and μ is the effective viscosity (sum of laminar and turbulent contributions). The turbulent viscosity is calculated through the solution of a standard k- ϵ model. The source vector in the momentum equation, S , includes the body forces, such as buoyancy, boundary effects and for solidification problems the Darcy source. The Darcy source represents the resistance to flow resulting from the presence of solid and is equal to

$$\frac{\mu}{K} \underline{u} \quad [3]$$

where K is the permeability calculated here using the Carmen-Kozeny equation:

$$K = \frac{f_L^3}{\zeta (1 - f_L)^2} \quad [4]$$

where f_L is the fraction of liquid and ζ is constant associated with the mushy region.

Heat transfer and solidification

The energy equation, with temperature as the dependent variable, is given by

$$\frac{\partial}{\partial t} (\rho c_p T) + \nabla \cdot (\rho c_p \underline{u} T) = \nabla \cdot (k \nabla T) + S_T \quad [5]$$

where k is the thermal conductivity and c_p is the specific heat. The source term, S_T contains the contributions from the boundaries and the effects of phase change. The energy released due to a change of phase can be expressed as:

$$S = - \frac{\partial}{\partial t} (\phi \rho_m f_L L) - \nabla \cdot (\phi \rho_m \underline{u} f_L L) \quad [6]$$

where L is the latent heat of solidification, ρ_m is the density of the metal and ϕ is the fraction of metal obtained from the free surface model.

The free surface model

The interface between the molten flux and the liquid metal is modelled using the scalar equation algorithm (5). The algorithm solves the equation:

$$\frac{\partial \phi}{\partial t} + \underline{u} \cdot \nabla \phi = 0 \quad [7]$$

for the metal volume fraction in an element, on a stationary mesh. Smearing of the interface is reduced significantly by solving equation [7] explicitly and using a van Leer advection

scheme. The continuity equation [2] is adjusted to provide an equation that represents volume conservation

$$\frac{D(\ln \rho)}{Dt} + \nabla \cdot (\underline{u}) = 0 \quad [8]$$

where D/Dt is the substantial derivative. Expressing the equation in this form removes the problems caused by the density discontinuity at the interface.

The Counter Diffusion Method for free surface tracking

The main practical problem in following a moving interface through a fixed mesh is that of maintaining a sharp property discontinuity. This is accomplished in the various traditional methods using specialised numerical schemes such as the Van Leer TDV scheme (7), the Level Set Method (8), or alternatively relying on a front sharpening/reconstruction scheme such as Donor-Acceptor (9). However, all these schemes are explicit, which means time-steps have to be small enough to satisfy the CFL criterion. This criterion is based on the residence time of the flow in any particular cell, which can be prohibitively small in fine mesh regions needed to characterise the relatively small instantaneous deformation of the slag/metal interface. Exceeding the CFL limit, generally leads to numerical instability and diverged solutions. To avoid this hurdle, and speed up the computation time a new time-implicit method for tracking the free surface was developed and implemented, the CDM (Counter Diffusion Method). This method can lead to dramatic improvements in time, since much larger time steps (by an order of magnitude) can be employed. As the name implies, the interface is allowed to diffuse, but then this diffusion is countered by gathering the spread in towards the interface. The main concept behind can be explained with reference to an air-water interface. Taking the interface to be at $\phi = 0.5$, any intermediate values of ϕ , ($0 < \phi < 1$) can be interpreted physically to signify the presence of either droplets ($0 < \phi < 0.5$) or bubbles ($0.5 < \phi < 1$). As during gravity separation, droplets re-join the liquid and bubbles re-join the gas. This 'sifting' can be achieved by prescribing a suitable slip velocity to separate real bubbles or droplets. The process is similar to diffusion, but operating against the scalar gradient, hence the term counter-diffusion. A counter diffusion 'flux' is computed for each internal cell face when the face belongs to an interface cell. The relevant flux is:

$$flux = C |R_{fvel}| (1 - \phi_{dn}) \phi_{up} \quad [9]$$

Where $C (= 4/3)$ is a scaling factor, R_{fvel} is the face-normal area velocity product, ϕ_{dn} and ϕ_{up} are downwind and upwind values of ϕ . With this formulation 'droplets' are pushed artificially back towards the liquid region; any gas in the liquid (bubbles) is then displaced automatically in the opposite direction by conservation. The factor $(1 - \phi_{dn})$ prevents sifting into completely full cells whilst ϕ_{up} ensures droplets are not taken from cells without liquid. The advantage of this method is that it can be used with any numerical scheme, and it can be implemented in both implicit and explicit formulations removing the strict CFL constraint.

CDM is still being evaluated, further developed and tested. Initial validation was carried out by comparison with the experimental study of a collapsing water column by J. -C. Martin and W. -J. Moyce (10). The positions of the water front and the residual of the water column are plotted (in non-dimensional coordinates) as functions of elapsed time and compared with the experimental data in figure 4 and figure 5.

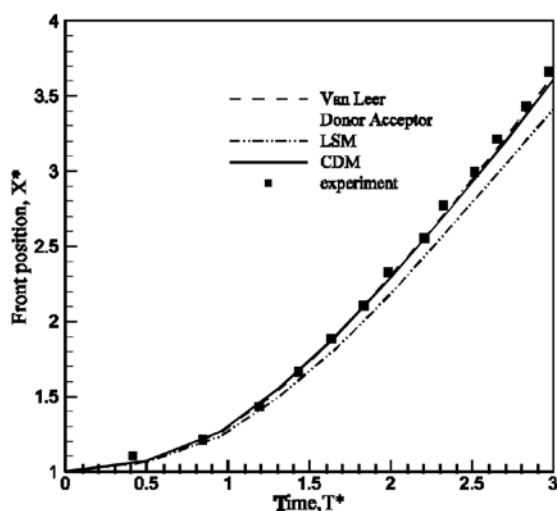


Fig. 4 - Comparisons of the numerical results with experimental results for the front position of the collapsing water column (10).

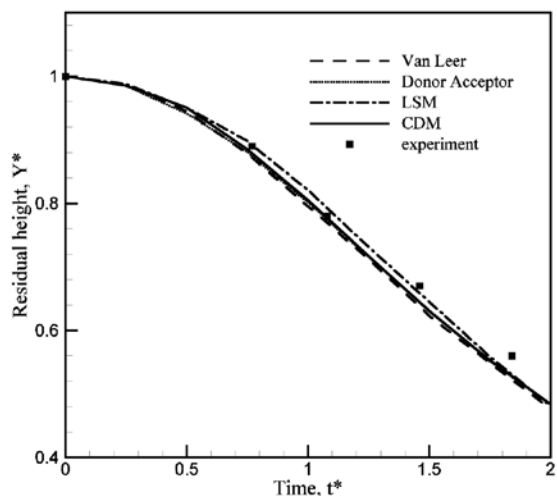


Fig. 5 - Comparisons of the numerical results with experimental results for the residual height of the collapsing water column (10).

It can be seen that there is very good agreement between the numerical results and the experimental data. Although in figure 4, the result with LSM is slightly less precise compared to the other methods, the general trends by the experimental data are obviously captured by all methods. From our perspective, more importantly comparisons of CDM can be seen from the point of view of efficiency as presented in table I.

It can be seen that CDM, being implicit, can be applied with a bigger time step ($CFL > 1$). Also, for the same time step, the number of iterations needed per time step is lower than that required by the other methods. The first two columns show that the time step for CDM could be ten times bigger than the others. With CDM, running time with $\Delta t = 0.1$ s is half that with a time step $\Delta t = 0.01$ s since more iterations within a time step are needed. But, even with the same small time step as others, the number of iterations within CDM is largely lower, seen in the last two columns.

The total running time with Van Leer is at least double that with CDM for the same time step and with the most popular Donor Acceptor method it is almost four times that of CDM. Finally, comparing the best possible time obtained with CDM, 16 s and Donor-Acceptor, 132 s for the same results, gives an impressive gain of a factor of 8.25!

TABLE I: Comparisons of the efficiency of CDM with other numerical methods.

Method	$\Delta t = 0.1$ s		$\Delta t = 0.05$ s		$\Delta t = 0.01$ s	
	N	t (s)	N	t (s)	N	t (s)
Van Leer	divergence		Breaking CFL		10	47
Donor Acceptor	divergence		Breaking CFL		40	132
Level set	divergence		Breaking CFL		20	121
Counter Diffusion	20	16	15	17	5	34
Δt = time step ; t = running time ; N = average number of iterations per time step						

Turbulence model modifications

Turbulence has an important role to play in these simulations, not just for its effect on the flow field, but for its role in heat transport to the solidifying shell but also to the flux layer. The current trend for simulating turbulence in continuous casting is by using the LES method (1, 3). However, this would lead to an increase in computational cost, so although LES models exist in PHYSICA, the standard k- ϵ model was adapted instead to our aim. It was observed both in our computations and in previous CFD computations performed by ArcelorMittal, that although surface oscillations were successfully predicted in air, the presence of an oil layer led to their almost complete suppression in contrast to experiments. The turbulence model was suspected for this behaviour. Two avenues were open to investigation: (1) The suitability of the k- ϵ model in transient simulations, (2) The effect of density change and interfacial energy on sub-grid turbulence at the interface.

The standard k- ϵ model is the one most widely used in many applications but it was born to describe steady

state problems. Its use in transient problems is acceptable, provided the time step used in the CFD simulation is not in the initially important range of flow-induced eddies. Should that be the case, turbulent energy is overestimated leading to excessive diffusion. This would suppress the energy governing surface oscillations and so leading to artificial damping. To overcome this deficiency and fill the gap between LES and standard RANS models, a 'filter' in the Kolmogorov-Prandtl equation has been introduced to reduce the effective viscosity, Johansen (11).

In general, when conducting fluid flow computations, it is desirable that the cell Reynolds number is not larger than $O(1)$ so that the flow structure can be satisfactorily resolved. If the eddy viscosity is excessive it will smear out the flow structures that are within the reach of a given grid resolution. Imposing a filter implies that all the turbulence structures smaller than filter size will not be resolved. The filter size is chosen according to the following expression

$$f = \text{Min} \left(1, \frac{\Delta \cdot \varepsilon}{k^{3/2}} \right).$$

Then, turbulent viscosity is given by:

$$\mu_t = C_\mu f \rho \frac{k^2}{\varepsilon}.$$

Δ is the filter size, which is related to the characteristic length of the problem, that is to the shear layers generating the turbulent structures in the flow. With increasing filter size the "filtered k-ε" model approaches the standard one. An advised filter size for symmetric wake flow is $0.075 L$, where L is characteristic length. This was determined by Johansen by comparing the vortex street behind a square obstacle with experimental measurements.

This adaptation of the k-ε model was implemented in PHYSICA for the continuous casting problem. The new version led to a dramatic change in the amplitude of surface oscillations and gave results that are more in accordance with experimental data, especially in the cases with an oil layer. Figure 6 shows the effect of the filter on the time variation of horizontal velocity for measurement point 3.

The filter value chosen for the simulation was related to the size of the SEN port diameter. The exact value used is a matter of experimentation, although the Prandtl Mixing Length value for a round jet was considered a good start. Figure 7 shows the effect of two different filter lengths (3 mm, 4.5 mm) on the amplitude of oscillation at various experimental positions.

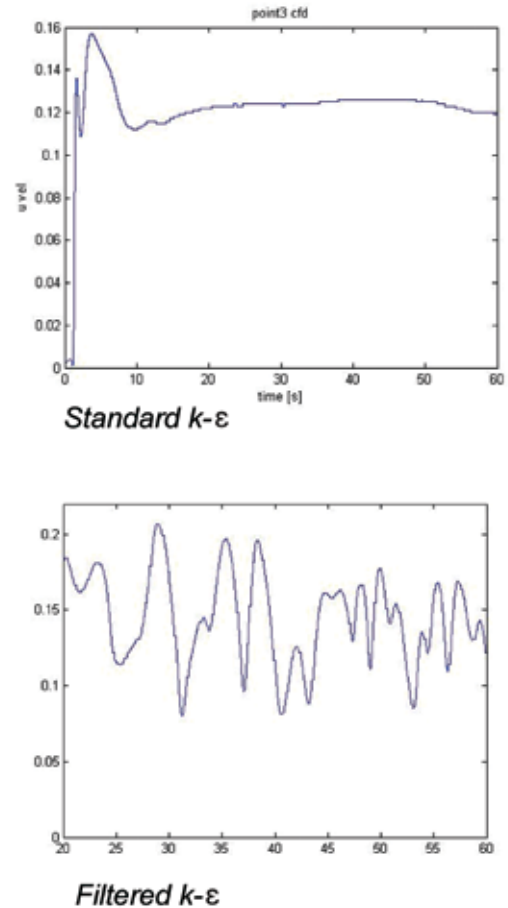


Fig. 6 - Horizontal velocity distribution point 3 (276,2.25,200) (simulation with 1cm oil, inlet velocity 1 m/s) showing the drastic effect of turbulence damping on oscillation amplitude.

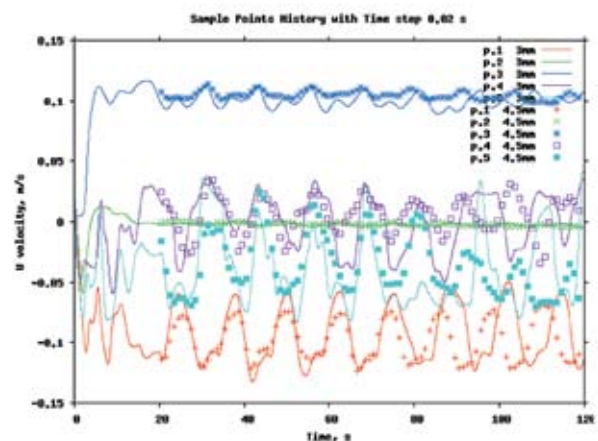


Fig. 7 - Effect of k-ε filter size on sub-surface velocity fluctuations (3 mm & 4.5 mm filters).

Although not explicitly stated in Johansen's papers, filter size and time step are related, since the period of oscillation is related to wavelength. The time step effect can be seen in figure 8 for two different time steps, 10 ms and 20 ms.

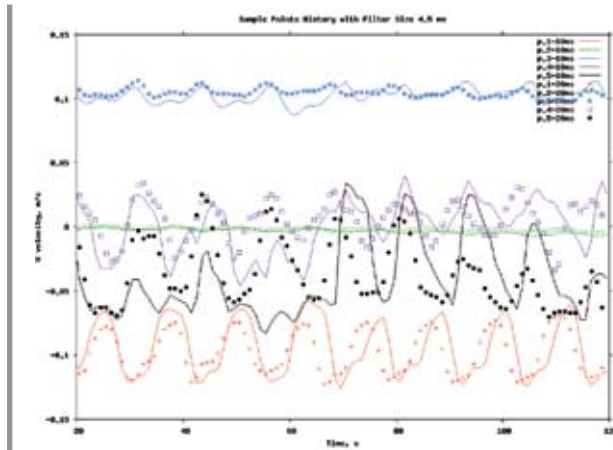


Fig. 8 - Effect of time step size on sub-surface velocity oscillations. Filter size 4.5 mm, $\delta t = 10$ ms & 20 ms.

Vertical velocity fluctuation damping needs to be introduced also at the interface between water and oil. This was done by suppressing the turbulence in zones where the gradient of density is high (buoyancy stratification of turbulence). Physically, the vertical component of turbulent kinetic energy k_z is reduced between the two fluids since any displacement in the z , or diminishing density direction will lead to a restoring buoyancy force. Studies in the literature (12) show that the energy lost is returned to the directions parallel to the interface. So, the energy lost needs to be re-distributed in the other two kinetic energy components, k_y and k_x . Focusing only on the fluid dynamics of the problem we can neglect this detail, but it is thought it may be an important factor in heat transfer at the interface as the turbulent kinetic energy influences the heat exchange coefficient. Figure 9 shows the effects of the buoyancy stratification of the turbulence combined with the effect of the filter on turbulence viscosity. The filter takes away turbulent energy that has already been accounted for in the NS equations, hence the overall level is reduced. Then, the buoyancy stratification effect produces damping of turbulence at the oil-water interface which can be seen in the top of the right-hand figure.

In analogy to fire modelling studies (13) the buoyancy stratification term is implemented through a sink term in the k and ϵ equations, which is proportional to the density gradient in the gravity direction.

Particle Tracking system

The particle-tracking model has some novel features (14), used to couple the particles to the mean flow through variation in the density field. The argon flow rate is split into a number of parcels each carrying an equal mass such that the total mass equals the required inflow. One particle is tracked for each parcel using

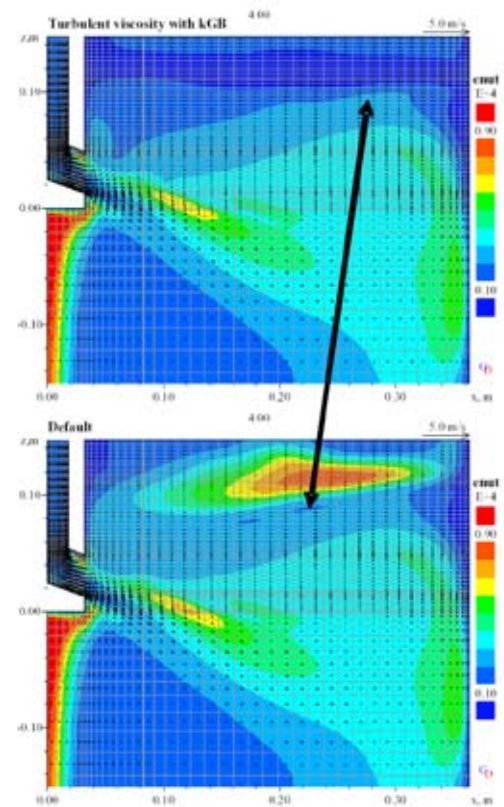


Fig. 9 - Contours of 'Enut' (turbulent viscosity). Above with buoyancy stratification plus filter, below filtered k- ϵ only.

a conventional Lagrangian method. The particle velocity, U_p is computed from:

$$U_p = (U_p + S_u * \delta t) / (1 + F * \delta t) \quad [10]$$

Where:

$$F = 0.75 * C_d * \rho * V_{slip} / (d_p \rho_p), \quad S_u = F * U_p + (\rho_p - \rho) * g / \rho_p$$

and $V_{slip} = U_p - U$

where the subscript p indicates particle values, other values are those associated with the metal, d_p is the diameter of the particle and g the gravity constant. The particle time step size, δt , is chosen so that a particle takes a specified number of steps to cross an element. Two methods were used to calculate the drag coefficient C_d depending on the size of the bubble, the Reynolds number and the Weber number. Details are given in (14). The particles are randomly seeded just inside the circular inlet. All particles are initially located within a radius of 37 mm from the centre of the inlet. The inlet has a radius of 40 mm. Particles are assigned an initial velocity of 2 m/s, close to the continuum velocity, and tracked until they reach the metal-flux interface or solid metal. The time a particle spends in an element, Δt , is recorded and the argon volume fraction of the element is increased by:

$$\Delta t (m_{ar} / N_p) / \rho_p \quad [11]$$

where m_{ar} is the mass flow rate of argon at the inlet and NP is the number of packets.

■ COMPUTED RESULTS

Several cases were studied, in particular to validate the model against water/oil experiments. Parameters considered include the oil layer thickness, casting speed (alternatively the SEN fluid velocity) and nozzle geometry. Some examples are given below.

Figure 10 compares a high flow rate case with 2 cm oil, but no gas. The experiment on the right, clearly demonstrates that the oil layer is pushed away from the side wall of the mould by the upper recirculation jet, leaving the water surface uncovered. At the same time, the oil is dragged into the water with the layer thickening and some instability appearing at the interface between them. The simulation shows a similar result, although there are differences in the actual profile.



Fig. 10 - The case with a 2 cm silicon oil layer.
The simulation displays the same characteristics as the experiment, including the formation of folds and the uncovering of the narrow end of the water.

Increasing the oil layer thickness as in figure 11 leads to the surface being recovered, but there is still evidence of shear induced break up of the interface due to the top jet action.

The flow pattern developed is shown in a fixed-interface, quarter-section computation of an actual caster in figure 12. The light liquid is now slag produced by the melting of liquid powder and the heavy liquid is steel. The upper and lower recirculation loops are clearly evident, plus the complex three dimensional nature of the flow in the upper part of the mould. The figure depicts the development of a solidifying skin surrounding the metal and also the top powder layer. Since the jets are hotter than the surrounding fluid, they seem to form an impression on the skin layer which is of non-uniform thickness.

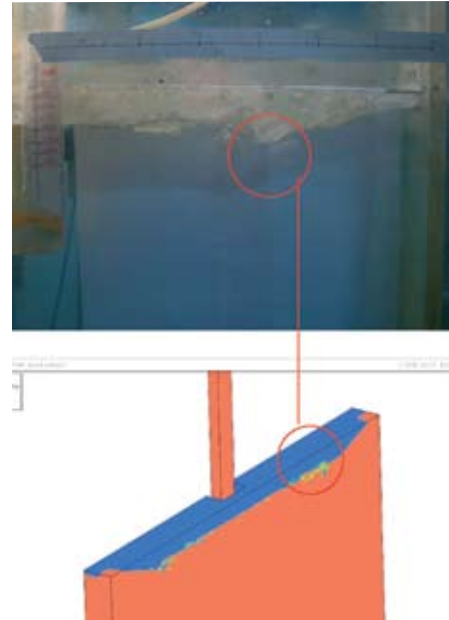


Fig. 11 -The water model case with a 3 cm oil layer covering.

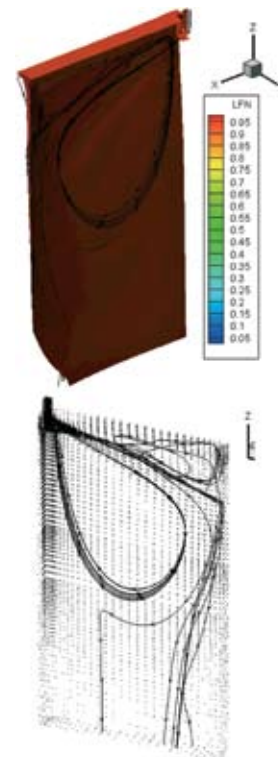


Fig. 12 - One quarter of the mould section with the upper and lower convection loops formed once the SEN jet reaches the narrow section wall. The path of the hot jet can also be detected in the solidifying skin shown on the left.

Figure 13 shows a water model simulation with a rectangular SEN and outlets. Time dependent simulations identify vortices at the oil-water interface, which appear to pull the lighter liquid, oil, into the water. The position of these vortices varies and can only be captured in a fine mesh simulation. Similar vortices appear in experiments.

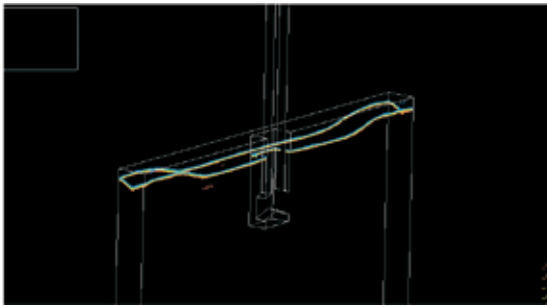


Fig. 13 - Presence of vortices which drag the lighter phase as droplets into the heavy phase, indicated by time dependent calculations.

Figure 14 shows the behaviour of bubbles as they enter the mould. The plots show contours of gas volume fraction and this simulation relates to a case without an oil layer on the surface. The Lagrangian model allows a mixture of bubble sizes to be prescribed, without coalescence or break-up allowed in the model at present. The plot shows some of the gas escaping straight to the surface on exit from the nozzle. This corresponds to the large bubbles, where buoyancy forces are dominant. Since the bubbles effectively change the volumetric density of the mixture, the SEN jets become shorter due to a reduction in momentum and also become more buoyant.

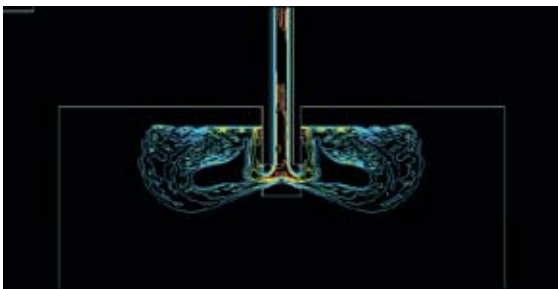


Fig. 14 - Gas concentration obtained for the case without an oil layer cover.

When an oil layer is added, then the question arises as to how the bubbles penetrate the surface, the delay imposed by interfacial tension to allow for film drainage and the amount of heavier fluid entrained in their path. Figure 15 illustrates this effect for two specific particle size streams, for diameters of 4 mm and 8 mm respectively. On the right, the time-averaged particle tracks are shown. There is clear separation depending on size, since the larger bubbles float straight up, whilst the smaller ones tend to follow the jet a bit longer. Where the interface is breached, the heavier fluid is entrained into the flux layer. At the moment this is a qualitative description, since the physics of film break-up are at present not accounted for in the model.

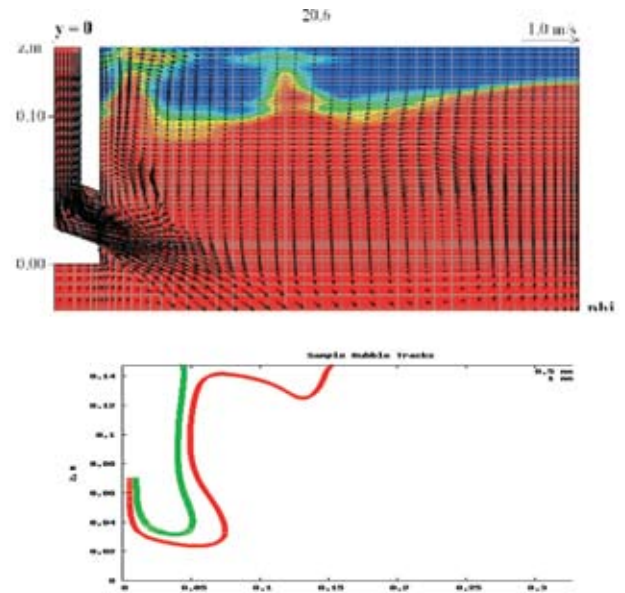


Fig. 15 - Entrainment of the heavy fluid into the lighter one, shown by time averaged bubble tracks. In this bimodal bubble distribution, large bubbles head straight towards the surface due to buoyancy, whilst smaller bubbles tend to follow the jet further before rising.

Figure 16 shows the shell thickness at the copper mould exit for different casting speeds. The shell thickness is taken to be the distance between the wall and the region where liquid fraction is 0.5. The validation data were obtained from Lopez (15).

The graph shows that the predicted value, 0.017 m at the mould exit ($z = -0.67$ m in the domain) is in good agreement with work in the literature. This thickness is the average thickness on the wide face for a casting velocity of 1.25 m/min.

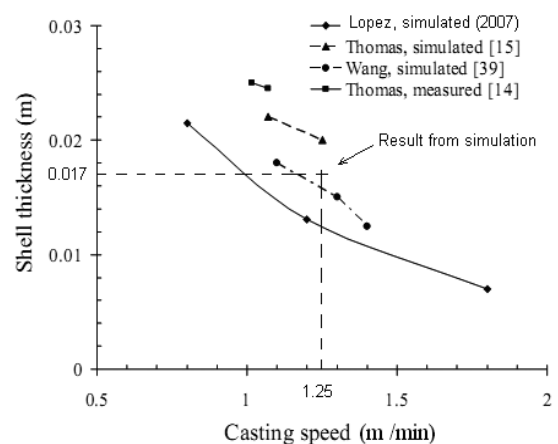


Fig. 16 - Comparison between predicted average skin thickness at the exit from the mould with experiments and other simulations from the literature.

Finally, figure 17 compares experimental water model frequency response curves for a case with 3 cm oil covering against several simulations. One of the simulations is for a 5 cm oil layer and shows significantly lower oscillation amplitudes. Two LDA points are compared, 'x3' close to the jet sensitive to jet oscillations and point 'x1' close to the oil/water interface, sensitive to interfacial waves. Although difficult to obtain point by point agreement, amplitudes are comparable in magnitude, with a significant low frequency content present, believed to be associated with the lower jet loop transport time. The simulations were limited in time due to computer cost and do not necessarily capture at this stage enough cycles of the signal at lower frequency for a meaningful FFT analysis.

CONCLUDING REMARKS

A main objective of this work has been to develop a complete fluid dynamics model of the continuous caster mould region, including the dynamic behaviour of the slag/steel interface. This model was developed by solving the source-balance transport equations for conservation of mass, momentum and turbulence kinetic energy. The model was validated against a water/oil physical model equipped with LDA velocity measurements and video recordings of interface position.

The results indicate that, mean surface profiles are generally correctly predicted with standard RANS turbulence models, but surface oscillations are damped when oil is present. Turbulence model modifications were introduced to account, (a) for transient filtering of wave numbers in the range of interest, (b) to account for sub-grid damping due to negative density gradient stratification.

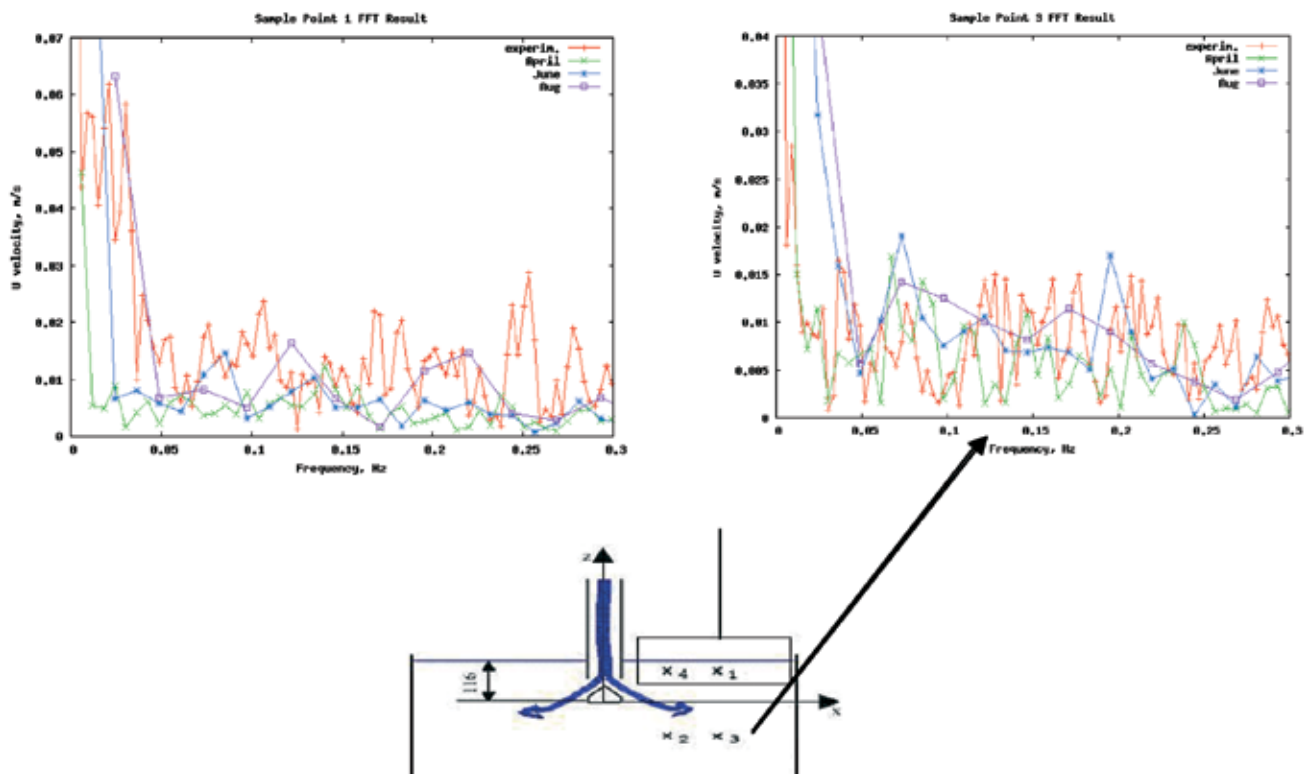
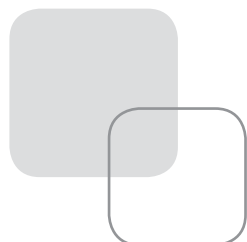


Fig. 17 - Frequency response at points x1 and x3, comparing experimental results against several predictions.

Full 3D simulations take several weeks to complete. A novel 'Counter-Diffusion-Method' algebraic slip model was introduced to allow implicit interface tracking calculations. Finally, oscillation amplitudes comparable to experiments were captured, including low frequency oscillations observed in the experiments. Experimental and simulation work continues.

A quasi-steady approach was used to simulate argon bubble tracks, which accounts for volume displacement and momentum exchange between gas and liquid through a mixture density approach. The argon gas has a significant influence on the SEN jets due to the added buoyancy and it also affects the behaviour of the interface. Once bubbles are allowed to penetrate the interface, they entrain liquid with them, resulting in enhanced mixing. Future work will introduce a delay mechanism, to account for the effect of interfacial tension on transit time as a function of bubble diameter.

Heat transfer calculations have been carried out using a fixed interface position. The results show melting of the flux powder and development of the skin layer, using experimental heat transfer coefficients. Predicted values of skin thickness and liquid slag thickness broadly agree with experimental measurements.



REFERENCES

- (1) THOMAS (B.-G.), ZHANG (L.) - Review: Mathematical modeling of fluid flow in continuous casting of steel», *ISIJ International*, vol. 41, n° 10, p. 1181-1193, 2001.
- (2) DOMGIN (J.-F.), GARDIN (P.) - Limitation of slag entrainment in tundish and reduction of ladle steel, *Sohn Int. Symp.*, TMS, 2006.
- (3) THOMAS (B.-G.) - Modeling of the continuous casting of steel: past, present and future, *Electric furnace conf. proc.*, vol. 59, ISS, Warrendale, PA, (Phoenix, AZ), 2001, 3-30, Pericleous (K., Croft (T.-N.), Garding (P.) et al. MCWASP IX 2005.
- (4) CROFT (T.-N.), PERICLEOUS (K.), GARDIN (P.) *ECCC Birmingham*, 2002.
- (5) ANAGNOSTOPOULOS (J.), BERGELES (G.) Three dimensional modelling of the flow and the interface surface in a continuous casting mould model, *Metallurgical and Materials Transactions B*, vol 30, p. 1095-1105, n° 6, 1999.
- (6) PHYSICA web address:
<http://staffweb.cms.gre.ac.uk/~physica/>
- (7) VAN LEER (B.) - Towards the ultimate conservative difference scheme, V. A second order sequel to Godunov's Method, *J. Com. Phys.*, 32, 101 - 136, 1979.
- (8) STANLEY (O.-J.), RONALD (F.-P.) - Level set methods and dynamic implicit surfaces, Springer-Verlag, ISBN 0-387-95482-1, 2002.
- (9) HIRT (C.-W.), NICHOLS (B.-D.) - *J. Comp. Phys.* 39, 201, 1981.
- (10) MARTIN (J.-C.), MOYCE (W.-J.) - An experimental study of the collapse of liquid columns on a rigid horizontal plane, *Phil.Trans.R.SOC*, vol. 244, n° 882, p.312-324, 1952.
- (11) JOHANSEN (S.-T.), SHYY (W.), JIONGYANG (W.) 2 filter-based unsteady RANS computations, *International Journal of Heat and Fluid Flow*, 2003.
- (12) ABDULMOUT (H.) - The flow patterns in two immiscible stratified liquids induced by bubble plume, *Inter. Journal of Fluid Dynamics*, vol. 6, Article 1, 2002.
- (13) MARKATOS (N.-C.) AND PERICLEOUS (K.-A.) An investigation of three-dimensional fires in enclosures, *Revue Générale de Thermique*, 266, 67-83, 1984.
- (14) CROSS (M.), CROFT (T.-N.), DJAMBAZOV (G.), PERICLEOUS (K.-A.) - Computational modelling of bubbles, droplets and particles in metals reduction and refining, *3rd Int. Conf. on CFD in the minerals and process Industries*, CSIRO, Melbourne, Australia, 2003.
- (15) RAMIREZ-LOPEZ (P.), LEE (P.-D.), MILLS (K.-C.), MORALES (R.-D.) - A coupled model to simulate the solidification inside the continuous casting slab mould, *Liquid Metal Processing and Casting Symposium 2007*, p. 133-138, 2007.